Study on Optical Combustion Sensor for Spark Ignition Engine

Y.Ohyama, H.Kuroiwa* and M.Ohsuga

Hitach Research Laboratory
2520 Takaba
Katsuta 312
Japan
* *Sawa Works*
Hitachi, Ltd.

ABSTRACT

An optical combustion sensor that combines fiber optics with a conventional spark plug, was investigated. This high-tech, compact in-cylinder combustion sensors consist of a 1-mm diameter quartz glass optical fiber cable inserted through the center of a spark plug. The tip of the fiber is machined into a convex shape to provide a 120-degree view of the inside of the combustion chamber.

Light emitted by the combustion flames in the cylinder is transmitted by optical cable to an opto-electric transducer. As a result, combustion rate, spark energy level and air-fuel ratio can be monitored. Its sensor would give more accurate readings of spark energy and air-fuel ratio than sensors designed to measure pressure inside the cylinder. Because it is integrated with a spark plug, the sensor is easily installed to multi-valve engines. Availability of the following sensings, such as knock, firing timing, misfire, maximum torque timing, flame temperature, spark intensity, air-fuel ratio, combustion pattern (diffused flame or premixed flame) is investigated using 4 cycle 4 cylinder, 1.8l spark ignition engines.

INTRODUCTION

The study of emissions from flames forms an important facet of combustion analysis, with implications for future engine control strategies. [1]~[6] Much works has been reported regarding luminous emission from spark ignition engines. Each combustion process in the engine consists of a propagating flame and luminous emission. The emission spectra from engine flames, the radiation at the end of each flame, the crank angle of a peak in radiant emission for air-fuel ratio and spark advance, and the air-fuel ratio can all be determined. The ability to avoid misfire in each cylinder by feedback air-fuel ratio control to minimize hydrocarbon emissions and cyclic variability, the ability to control during transient operation, and the ability to make spark timing adjustment to minimize nitrogen oxides emissions or knock has been proposed using an optical combustion sensor. A spark plug integrated optical combustion sensor, which can provide more versatility than provided by more conventional pressure sensors, is described. It can be used for the purpose of combustion analysis and feedback engine control.

EXPERIMENTAL ASPECTS

Optical Combustion Sensor

An optical combustion sensor that combines fiber optics with a conventional spark plug, was investigated. This high-tech, compact in-cylinder combustion sensors consists of a 1-mm diameter quartz glass optical fiber cable (core, 0.9 mm) inserted through the center of a spark plug, as shown in Fig. 1. The tip of the fiber is machined into a convex shape to provide a 120-degree view of the inside of the combustion chamber. The sensor is designed to stay free of deposits from combustion products and cracked lubricant. During tests, loss in sensitivity due to deposits was 5% and no problem of durability was encountered with ultrasonic cleaning.

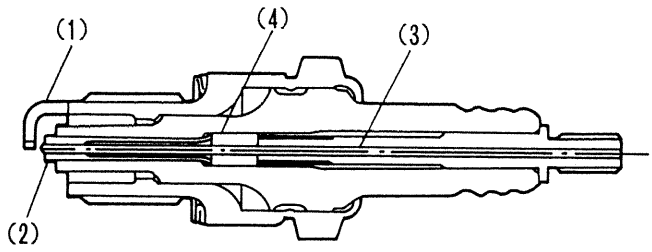

Fig. 1 Spark plug integrated optical combustion sensor
(1) Outer electrode
(2) Center electrode
(3) Quartz glass fiber
(4) Glass seal

The tips used are shown in Figs. 2(a) and (b). One is a projected type and the other is embedded into the center electrode. Fig. 2(c) shows another electrode configuration with a gap of 0.8 mm. The view fields of the sensor measured with a standard light source are shown in Fig. 3. The sensor is installed in the cylinder head where the combustion process can be viewed.

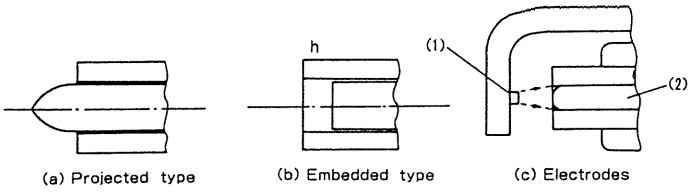

Fig. 2 Tips and electrodes of the sensor
(1) Pt tip
(2) Quartz glass fiber

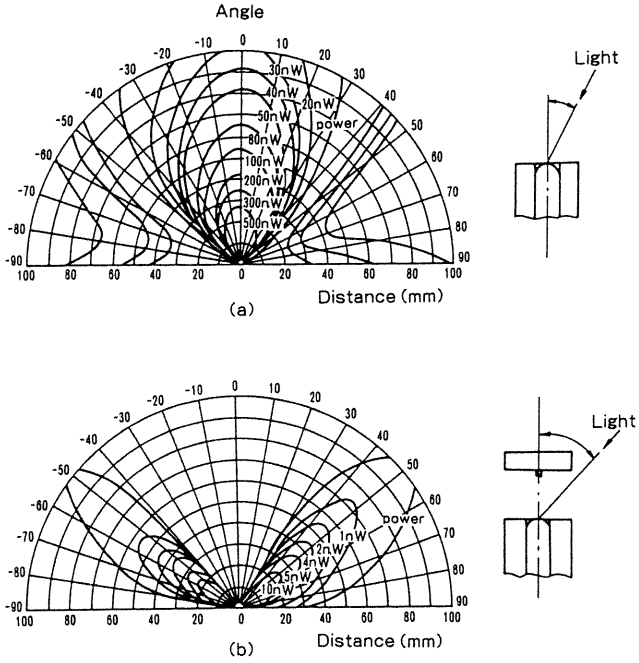

Fig. 3 View fields of the sensor

Measuring System

The design of the measuring system is shown in Fig. 4. The engine used is a conventional 4-cylinder, 4-cycle 1.8L spark-ignition unit. As shown in Fig. 4, light and flame luminosity are passed from the combustion chamber through the sensor and along the fiber optical cable into a monochrometer or a photo transistor, which converts the optical signal to an electronic one.

Fig. 5 shows the transmission loss of the optical bundle, together with the quartz glass fiber used. The slit dimensions of the monochrometer are 10 μm x 3 mm x 1200, with wavelength accuracy of $\pm$0.1 nm. A photomultipler with a peak response at 450 nm is used, and the sensitivity range is from 200 to 1400 nm. The sensitivity range of the NPN planar silicon phototransistors used is 450 - 1150 nm. The peak response is at 800 nm. The output voltage to luminosity ratio is 10V/(60mW/cm^2). The time constant for the step response is 300 - 350 ns. Although the optic cable transmission losses are high, the total light transmission loss is still dominated by that due to carbon build-up on the sensor tip. Satisfactory operation is demonstrated at low idle, which is the weakest signal source.

The system included a 12-bit A/D converter for cylinder pressure and luminosity data

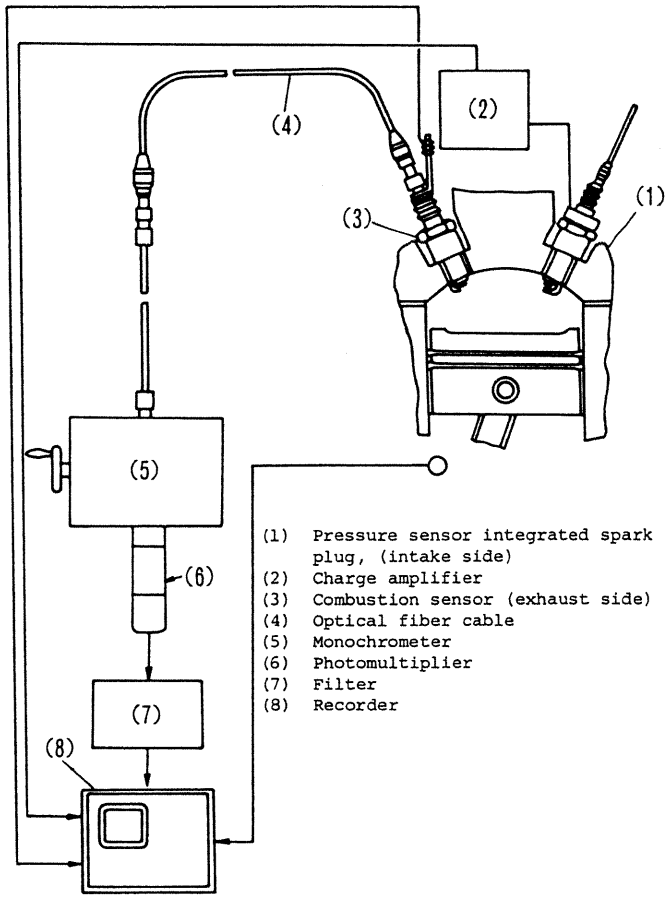

Fig. 4 Experimental equipment

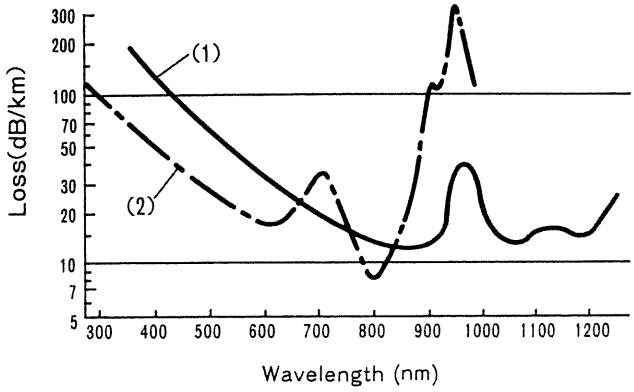

Fig. 5 Optical transmission losses
(1) Glass optical bundle
(2) Quartz glass fiber

aquistion. It is capable of sampling 8 channels of data every 0.25 degrees of a crank rotation for a total of 350 consecutive engine cycles. It has 8 Mbyte of memory available for storage.

Engine Tests

In order to evaluate the performance of the sensors, engine tests were run to compare the signal with combustion pressure sensors.
Key engine parameters are:

· Compression ratio	8.8
Bore, mm	83
Stroke, mm	83.6
· Displacement, L	0.452 x 4 cylinders

Exhaust concentrations of carbon monoxide, unburned hydrocarbons, nitric oxide, carbon dioxide, and oxygen were measured and used to compute air-fuel ratios based on carbon balances. In-cylinder pressure data were also obtained.

BASIC CHARACTERISTICS

Effects of Pressure on Signal Output

The change in power meter output against the standard light source is less than 6% as the pressure on the sensor tip is statically changed in the range of 0 - 5.7 MPa. The gap between the light guide of the light source and the tip of the sensors is 2 - 10 mm. The increase in the output is small because the angle of the light emitted from the guide decreases slightly from 20 to 19.72° due to the change in refraction by the increase in pressure. There is no change in the signal against the stepwise change in pressure from 0 to 5.1 MPa.

Drifts and Degradation of Sensor

As show in Fig. 6, the zero point drift apt to increase as the spark timing increases, because of the temperature rise of the sensor tip deposits. The drift is similar to the output of the tip when the tip temperature is 800 - 900°C. Periodically the engine was stopped, the sensor was removed and its attenuation and transmission efficiency were measured. A key feature for satisfactory sensor operation is the opacity of the tip at the combustion face. In order to avoid excessive carbon build-up, the minimum operating temperature should be maintained above the temperature for electrode self cleaning. Above this temperature the carbon becomes friable and can be removed by gas flow across the tip. The transmission efficiencies during idling decrease rapidly when the mixture is rich, as shown in Fig. 7. In going to lean mixture operation at partial load after extended idling as shown in Fig. 7, the sensor can burn off excess carbon build-up in a matter of minutes. Self cleaning of the sensor tip maintains a low optical attenuation at partial and full loads.

Fig. 8 shows the transmission efficiency at partial load, together with the attenuation. The attenuation is less than 14%, which is smaller than the loss of the transmission efficiency

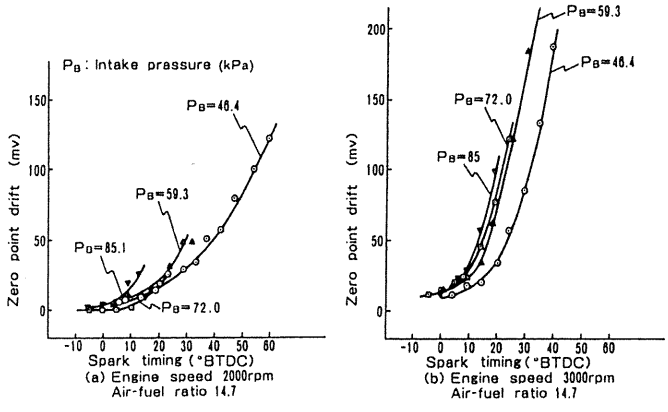

Fig. 6 Zero point drifts

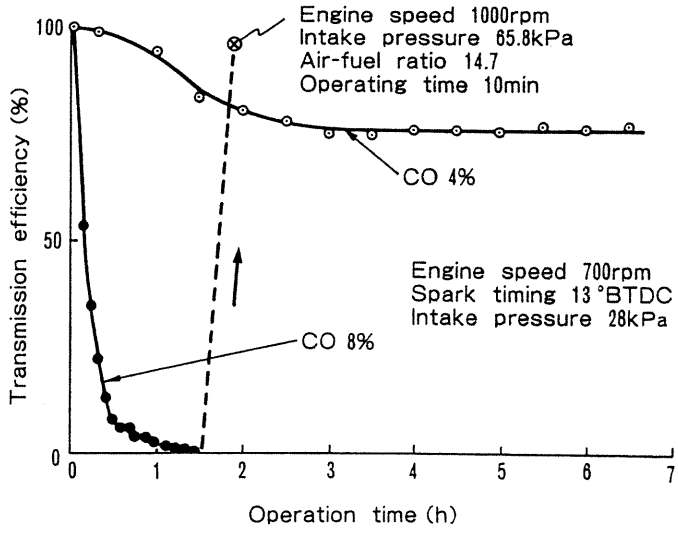

Fig. 7 Transmission efficiency during idling

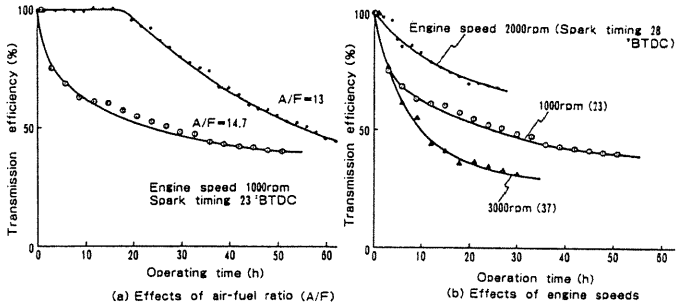

Fig. 8 Transmission efficiency at partial load

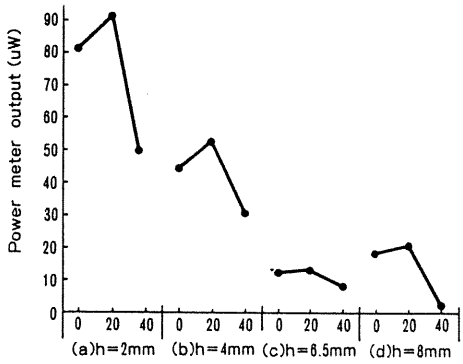

Fig. 9 Power meter output of embedded type sensor

measured with a standard light source and power meter. The level during this time does not increase after the initial 30 - 40 hours. Then it becomes a function of the engine operating mode just prior to the measurements. The deposits were measured by energy dispersion X rays and wave-length dispersion X rays. They include P and Ca, which seem to come from hydrocraking of lubricant.

Fig. 9 shows the power meter output of the embedded type sensor. The intial output decreases as the depth h shown in Fig. 2(b) increases. But the decrease in the output tends to be minimized at h of 6.5 mm.

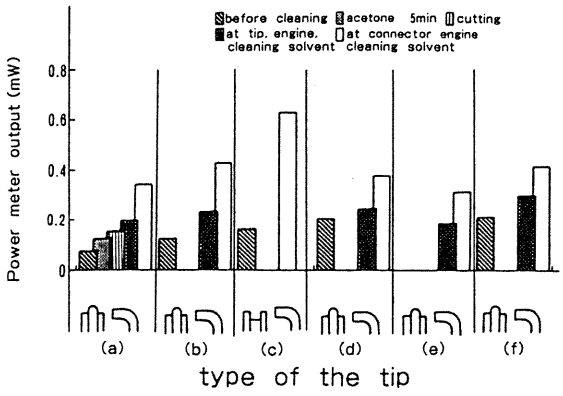

Fig. 10 Power meter output before and after ultrasonic cleaning

Fig. 10 shows the power meter output of the sensors before and after ultrasonic cleaning. Cleaning in acetone, cutting and cleaning in engine cleaning solvent were investigated. The transmission efficiencies are recovered to above 92% in most cases.

Effect of Location of Sensor

As shown in Fig. 4, the sensor can be fitted to the intake side and exhaust side of the cylinder head. The signal traces of installed sensors are shown in Fig. 11, when the exhaust side installed spark plug was ignited. The output of the intake side is delayed compared with the exhaust side, due to flame propagation. The delay time is about 1.2 m/s, so the velocity of the propagation is 33 m/s, for the distance of 40 mm. Another tests shows ignition delay time is 1.5 ms for the intake side and 2.0 ms for the exhaust side, for the engine speed of 2000 rpm, the air-fuel ratio of 14.7, the spark timing of 35°BTDC and the intake pressure of 85 kPa. The flame kernel formation of the exhaust side is delayed slightly compared with the intake side. But flame propagation of the exhaust side is faster. Then the crank angle for peak signal is the same as the intake side. The flame kernel formation of the exhaust side is faster for the engine speed of 2000 rpm, the intake pressure of 72 kPa, and the same for wide-open throttle conditions.

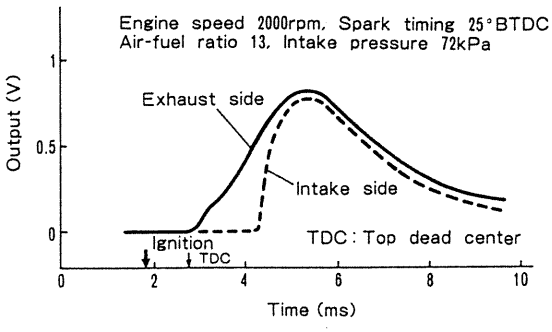

Fig. 11 Traces of the sensor signal

OVERALL EMISSIONS

Start of Combustion

The crank angles from the start of spark to the start of combustion for engine speeds of 1000, 2000, 3000 rpm and the air-fuel ratio of 14.7 are shown in Fig. 12. The start point of combustion is the same as that of the combustion pressure sensor; sensor lag to the true point is negligible. By optically sensing the start of combustion, a closed loop system based upon the final event can be achieved. The start of combustion is found to fluctuate from cycle-to-cycle by ± 5 crank angle engine degrees during steady state running. The timing was averaged over several readings to provide an accurate target.

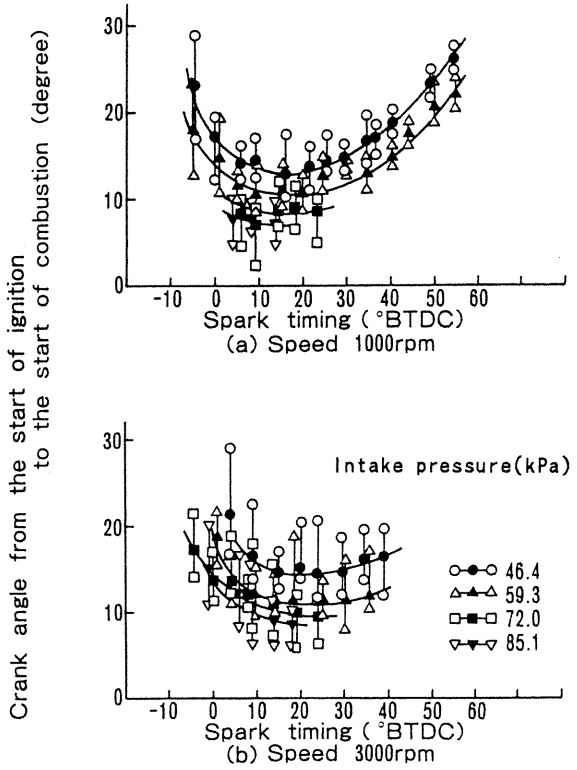

Fig. 12 The crank angle from the start of spark to the start of combustion

Overall Emissions

Overall emissions measured by the sensor and cylinder pressure for the engine speed of 2000 rpm, the air-fuel ratio of 17, and the spark timing of 22°BTDC are shown in Fig. 13. The signal at wavelength of 450 nm lags the pressure sensor signal by $\Delta t_1 = 0.1$ ms. The signal at 750 nm lags the pressure sensor signal by $\Delta t_2 = 0.4$ ms. These imply that the sensor is sensing some of the black body radiation resulting from the heating effect of the premixed burning. In some cases, the radiation resulting from diffusion burning becomes dominant late in the cycle. The relation between the output of the combustion pressure sensor P and that of the optical combustion sensor F is $F=kP^4$.

The wavelength band of 450 nm is not strongly influenced by black-body emissions from the combustion chamber walls. The emission is probably due to thermal emission of H_2O, a production of combustion, and radicals of C and CH. The fact that emission persists after heat release is also attributed to the fact that hot H_2O and particules continue to be emitted in the burned-gas region. The emission signal is zero during the compression process, unlike the cylinder pressure signal. For this condition, a weak luminosity emission is evident at the spark location, followed by negligible emission.

Fig. 14 shows the CH radical signal output at 431.5 nm wavelength for the engine speed of 2000 rpm, the air-fuel ratio of 15 and the intake pressure of 72 kPa. These are typical traces taken at partial load. The premixed radical reaction (1) and burning modes (2) are indicated on the traces. The emission by the CH radical at the spark location is evident in the initial stage. Then the signal output decreases slightly and recovers by thermal emissions.

The time lags, Δt_1, Δt_2 are shown in Fig. 15. As Δt_2 is shown, the peak signal of 750 nm

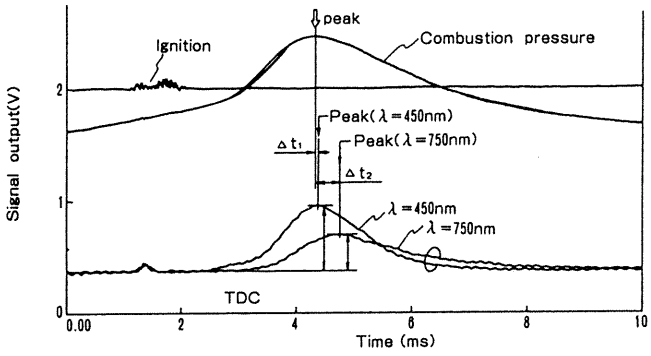

Fig. 13 Traces of combustion pressure and optical combustion sensor

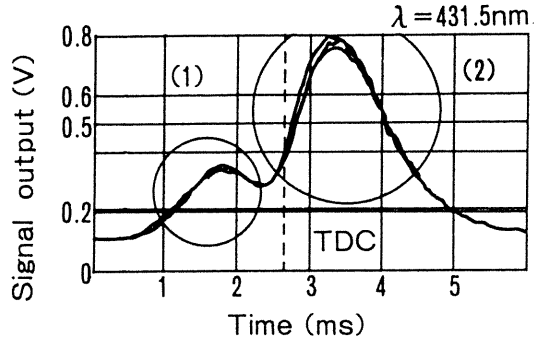

Fig. 14 Reproducibility of signals after averaging (Sample number : 100)

(1) Chemi-luminescence by CH radical
(2) Flame by thermal emission

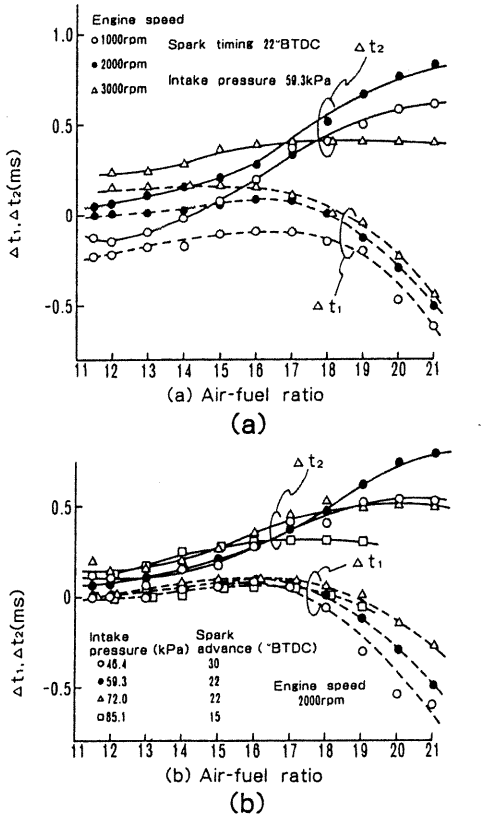

Fig. 15 Time lag of emission signal peak to pressure sensor

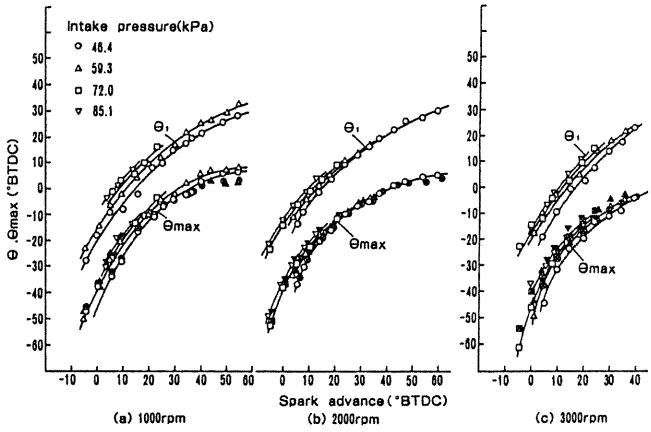

Fig. 16 Crank angle of start of combustion θ_1 and peak θ_{max}

wavelength lags behind the pressure sensor signal as the air-fuel ratio increases. There is no lag in the pressure sensor signal for the peak signal of 450 nm. Fig. 16 shows the crank angle at the start of combustion θ_1 and that of the peak of the signal, θ_{max} . As shown, θ_1 and θ_{max} increase as the spark timing advances. The engine torque is a maximum when θ is -10 to -15°BTDC.

SENSING AND CONTROL

Sensing

One possible use of the optical combustion sensor is for combustion analysis. The study of flame emission is an important part of combustion analysis. The sensing items are summarized in Table 1.

Table 1 Sensing items

Sensing items	Detecting methods
Knock	detecting the signal fluctuation
Misfire	detecting the intensity cycle by cycle at idling
Temperature	detecting the ratio of two wavelength signals
Start of combustion	detecting the trace of signals
Spark discharge	detecting the signal at spark discharge
Air-fuel ratio	detecting the ratio of two wavelength signals
Diffusion flame	detecting the signal trace during cycle
Crank angle of peak in signal	detecting crank angles of 13–15°ATDC for maximum torque

Control

Another possible use of the sensor is as one of the components used in future real time electronic engine control as shown in Fig. 17. For spark-ignition engines, a feedback system has been suggested using an optical sensor for control of cyclic fluctuation due to misfire (1),(2). The value of light emission for feedback engine control has yet to be demonstrated.

Closed-loop control offers the promise of tuning individual cylinders for optimum performance and emissions, better control of transient conditions, control over a wider range of air-fuel ratios, control of knock, and detection of misfire and diffusion burns. An alternative to pressure transducers or ionization probes is the optical sensor. Recently, optical sensors have been proposed to control the start of combustion in diesel engines. One possible use of the optical sensor described here is for achieving better cylinder-to-cylinder balance in conventional engine control systems. Control of individual cylinder torque by detecting the crank angle of the peak in signals, and then making adjustments to spark timing and fuel flow rate would lead to increased cyclic efficiency as well as a smoother running and quieter engine operations. By detecting the start of combustion and the crank angle of peak in signals, spark timing can be adjusted to maximize combustion efficiency at a given air-fuel ratio by operating each cylinder at near-MBT (minimum spark advance for best torque) timing. Adjustment of spark timing to minimize NO emissions or knock may be possible by detecting parameters as shown in Table 1.

More sophisticated control strategies may also be feasible. Control during cold start transient operation may be achieved by using the sensor from a small number of each cycle. During warming-up, control of individual cylinders may be required because operation occurs very close to the lean misfire limit. The ability to avoid misfire in each cylinder by feedback air-fuel ratio control should help to minimize hydrocarbon emission and cyclic variability. The conventional optimizer takes 80 s for optimum spark timing. But the optical sensor takes only two or three cycles for it. When the exhaust gas recycle rate increases, and the swirl ratio decreases, the peak crank angle is delayed. Then, these can be controlled by detecting the angle. The peak is the signal about temperature, so the exhaust gas recycle rate can be controlled.

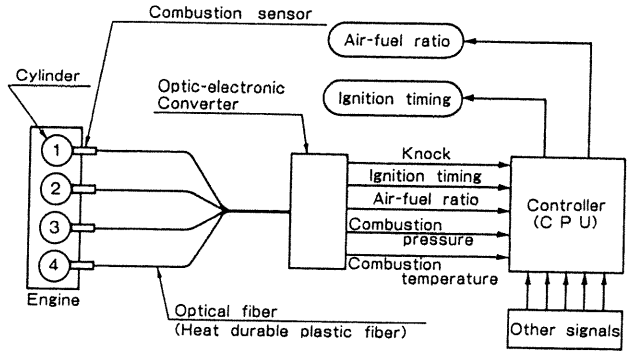

Fig. 17 Concept of engine control system using optical combustion sensor

SUMMARY

An optical combustion sensor that combines fiber optics with a conventional spark plug has been developed. Results obtained over a wide range of engine operating conditions show the following:

(1) The start of combustion, the crank angle of the peak in the emission signal can be directly detected from measurements. The other related information, such as knock can be predicted.

(2) In addition to combustion analysis, the ability to relate measured signals to knock, misfire, temperature, start of combustion, spark discharge, air-fuel ratio, diffusion flame, and crank angle of peak in luminosity signal suggested that an optical sensor of this type could be used in a feedback engine control strategy to improve fuel economy and lower exhaust emissions.

ACKNOWLEDGEMENTS

The authors thanks T. Saito, N. Ichikawa, S. Ueno of Sawa works for their contributions and supports to the design and development work.

References

(1) T. Sasayama, et al., Recent Developments of Optical Fiber Sensors for Automotive Use, Fiber and Integrated Optics, Vol. 7 (1988)

(2) T. Sasayama, et al., Recent Developments of Optical Fiber Sensors for Automotive Use, SPIE Vol. 840 (1987)

(3) D.J. Remboski, et al., Optical Sensors for Combustion Analysis and Control, Automotive Engineering, 97-6 (1989.6)

(4) J. Mallog, M. Kluting, Einsatz moderner Meßverfahren zur Analyse and Optimierung der ottomotorischen Verbrennung, MTZ 50-6 (1989)

(5) E. Day, et al., Start of Combustion Sensor, SAE Paper 890484 (1989)

(6) D. Nutton, R.A. Pinnock, Closed Loop Ignition and Fueling Control Using Optical Combustion Sensors, SAE Paper 900486 (1990)